The University of Tehran Press

Pollution

Print ISSN: 2383-451X
Online ISSN: 2383-4501

https://jpoll.ut.ac.ir/

Electrospun Nanofiber Membranes from Recycled Acrylic for High-Salinity Brine Desalination via Air Gap Membrane Distillation

Safa Naser Mohammed | Basma Ismael Waisi

Department of Chemical Engineering, College of Engineering, University of Baghdad, P.O. Box 47024, Baghdad, Iraq

Article Info

Article type:
Research Article

Article history:
Received: 16 May 2025
Revised: 31 August 2025
Accepted: 09 February 2026

Keywords:
Recycled acrylic
Brine desalination
Membrane Distillation
Electrospinning

ABSTRACT

This study reports the fabrication and performance evaluation of electrospun nanofiber membranes made from recycled acrylic (polymethyl methacrylate (PMMA)) for use in air gap membrane distillation (AGMD) systems targeting high-salinity brine desalination. Scanning Electron Microscopy (SEM) confirmed that the membranes possessed a uniform, highly porous nanofibrous structure with interconnected pores conducive to vapor transport. Atomic Force Microscopy (AFM) revealed a rough surface morphology, while water contact angle measurements exceeding 121° indicated excellent hydrophobicity, critical for effective liquid, vapor separation. Fourier-transform infrared spectroscopy (FTIR) verified the preservation of key ester functional groups, confirming the chemical integrity of the recycled acrylic. Performance testing was conducted under various feed temperatures (45–65 °C), flow rates (0.2–0.4 L/min), NaCl concentrations (35–140 g/L), and air gap distances (6–9 mm). The membranes achieved a maximum flux of 9.2 kg/m²·h at 65 °C and 0.4 L/min. As expected, higher salt concentrations reduced flux due to lower vapor pressure and increased concentration polarization. Despite variations in operating conditions, salt rejection consistently exceeded 99.994%, demonstrating excellent selectivity and operational stability. These results highlight the potential of recycled acrylic-based nanofiber membranes as a sustainable and high-performance solution for brine desalination using AGMD.

Cite this article: Naser Mohammed , S., & Ismael Waisi, B. (2026). Electrospun Nanofiber Membranes from Recycled Acrylic for High-Salinity Brine Desalination via Air Gap Membrane Distillation. *Pollution*, 12(1), 153-166. https://doi.org/10.22059/poll.2025.395374.2937

 Publisher: The University of Tehran Press.
DOI: https://doi.org/10.22059/poll.2025.395374.2937

INTRODUCTION

The rapid increase in the world's population, along with rising living standards and expanded industrial and agricultural activities, has led to a growing global demand for fresh water. About the year 2000, this demand was approximated at around 4000 billion cubic meters, and it is expected to rise by more than 58% by 2030 (Fernandes et al., 2025). In developing countries, there is an even sharper rise in water demand, with water demand projected to increase by above 93%, far exceeding the growth rates in developed regions. The maximized demand for clean water, coupled with limited freshwater resources, underscores the urgent need for efficient technologies capable of producing potable water from saline sources (Shahzad et al., 2019). The same as various desalination techniques, membrane distillation (MD) has gained increasing attention because of its relatively simple design and its ability to operate effectively at moderate temperatures, typically between 45 and 85 °C.

Unlike conventional desalination methods, MD tends to be less subject to membrane fouling and scaling. Consequently, it generally requires less intensive feed water pretreatment (Abid et al., 2023). Also, MD systems function under low pressure, which contributes to reduced equipment and operational costs (Soumbati et al., 2025). The basic principle of MD involves

*Corresponding Author Email: *basmawaisi@coeng.uobaghdad.edu.iq*

a vapor pressure gradient across a hydrophobic microporous membrane. That membrane enables available water vapor to pass, although it avoids the transmission of water liquid (Criscuoli, 2021). an encouragement of advances in this region includes the improvement of the MD membranes that are useful for electrospun polymeric nanofibers. These fibers offer several benefits, including a high surface-area-to-volume ratio, tunable surface characteristics, mechanical robustness, and chemical flexibility, all of which contribute to enhanced water vapor transport and improved overall membrane performance (Huang et al., 2003). Due to its features, electrospun membranes were discovered to have applications beyond desalination, such as in drug delivery systems (Abdulhussain et al., 2023), emerging energy technologies (Islam et al., 2019), water splitting (Zhang et al., 2022), smart packaging (Zhang et al., 2023), chromatography (Chigome et al., 2011), and wastewater treatment (Alkarbouly and Waisi, 2022).

For a successful MD operation, membranes must exhibit certain critical properties. This high hydrophobicity resists wetting, low tortuosity and thermal conductivity to ensure efficient vapor flow and reduce heat loss, and thermal and chemical stability under harsh conditions. These polymers have been electrospun to meet these demands, such as polypropylene (PP) (Fang et al., 2012), polyvinylidene fluoride (PVDF) (Albiladi et al., 2023), and polytetrafluoroethylene (PTFE) (Defor and Chou, 2024). Incorporating recycled Perspex, a commercial type of polymethyl methacrylate (PMMA), into membrane production has environmental and economic benefits. The perspex is a common thermoplastic with high transparency, mechanical strength, and chemical resistance (Ali et al., 2015), giving it an excellent choice for membrane applications. Recycling this material not only lowers plastic waste and pollution, however; it also provides a low-cost alternative to virgin polymers, which contributes to membrane fabrication. This study encourages a circular economy strategy by reusing post-consumer acrylic waste, while also meeting the worldwide need for economical and high-performance materials in water treatment technology.

The electrospinning provides several advantages over more traditional membrane fabrication techniques, such as melt spinning, sintering, and phase inversion. It allows the occurrence of ultrafine fibers at room temperature application of a high-voltage electric field (Liu et al., 2023).

The electrospinning method has been extensively adopted to fabricate different polymeric membranes from various precursor polymers. The PVDF nanofiber membrane was utilized for DCMD configurations, giving promising results with a stable water flux of about 21 kg/m²·h, which was obtained when the concentration of NaCl in the feed water was 3.5% NaCl solution at 50°C, and with water contact angles greater than 135° (Liao et al., 2011). In another study, a dual-layer membrane consisting of electrospun structural PVDF nanofibers and active top electrospun polymethyl methacrylate (PMMA) nanofibers (25% and 75% PVDF, respectively) was explored. The rejection salt and water flux of this membrane were 99.76% and 44.2 kg/m²·h, respectively (Safi and Waisi, 2023).

The current study describes the preparation of an innovative electrospun nanofibrous membrane from melted recycled acrylic (PMMA) for air gap membrane distillation (AGMD) to meet the continuous need for membranes, which are high-performing, cheap, and eco-friendly. Through appropriate tuning of the polymer solution composition and process parameters, researchers were able to achieve bead-free and defect-free fibers, suggesting a stable electrospinning process and a uniform fiber formation. The morphology was investigated by scanning electron microscopy (SEM) for surface morphology and atomic force microscopy (AFM) for surface topography, while surface hydrophobicity was determined by water contact angle (WCA) measurements and chemical composition using Fourier transform infrared (FTIR) spectroscopy. The permeation performance of these membranes was further studied under different operating conditions of AGMD, including feed temperature, feed flow rate, salt concentration in the feed, and different AG thicknesses. The findings described in this report

have great potential to assist in the sustainable development of desalination applications.

MATERIALS AND METHODS

Waste acrylic material was used, primarily composed of polymethyl methacrylate (PMMA) and commercially known as *Perspex*, which was collected from an advertisement shop. it is a rigid thermoplastic commonly used as a glass alternative in windows, eyeglasses, and aquariums. The organic solvents N,N-Dimethylformamide (DMF) (density: 0.948 g/cm^3) and Chloroform ($CHCl_3$) (density: 1.49 g/cm^3) were supplied by Alfa Aesar and used to dissolve the recycled acrylic. Sodium chloride (NaCl), purchased from Sigma-Aldrich, was used to prepare the saline (brine) feed solutions for the membrane distillation experiments to evaluate the membrane performance.

The recycled acrylic-based nanofiber membranes were fabricated using the electrospinning technique, as described in (Safi and Waisi, 2023). Initially, rigid acrylic plastic waste was ground into smaller fragments using an electric grinder. The resulting powder was first dissolved in chloroform ($CHCl_3$), followed by the gradual addition of N,N-dimethylformamide (DMF). The mixture was stirred magnetically at room temperature for 5 hours to ensure complete dissolution of the polymer and to obtain a homogeneous spinning solution (Subbiah et al., 2005). The uniform polymer solution was then placed in the 5 mL syringe, which was connected to a syringe pump for electrospinning. The solution was pumped with a flow rate of 2 mL/h, with a 13 cm distance between the dispenser tip and the collector. Electrospinning was started with a high voltage of 18 kV, and the polymer jet was extruded by a 21-gauge needle (21 × 1½″). The fibers were gathered on a rotating drum to generate a fibrous nonwoven web of about (13 by 30 cm). The relative humidity was kept at 20% during the procedure. After fabrication, the membranes were allowed to dry with solvent vapor loss minimized by using room temperature. Finally, the membranes were dried and kept in clean plastic containers to avoid contamination before characterization and testing (Navarro-Tovar et al., 2025).

Several numbers of analytical techniques were employed to investigate the physical, chemical, and surface characteristics of the fabricated membranes. The Scanning Electron Microscopy (SEM) (National Institutes of Health, USA) was utilized to capture high-resolution images of the surface morphology and topography of the recycled acrylic (RA)-based nonwoven nanofiber membranes, using a focused electron beam to reveal fine structural details. To ensure the chemical composition, Fourier Transform Infrared Spectroscopy (FTIR) (Spectrum 1800, Shimadzu, Japan) was carried out. This identifies a functional group technique by determining molecular bond vibrations, effectively providing a molecular "fingerprint" unique to the material (Coates, 2000). Surface roughness and nanoscale features were examined using Atomic Force Microscopy (AFM) (SPM AA300, Angstrom Advanced Inc., USA). The AFM estimated three-dimensional surface maps and valuable insights into fiber morphology and pore distribution across the membrane surface. The hydrophobicity of the membranes was evaluated through water contact angle (WCA) measurements, conducted using a goniometer (Theta Lite TL101, Biolin Scientific, USA). Images were analyzed using dedicated software to determine the contact angle by A small water droplet was carefully placed perpendicular to the membrane surface. This method remains a reliable approach for assessing surface wettability and hydrophobic character. All characterization procedures were performed at room temperature (approximately 20 °C) under standard ambient laboratory conditions.

A schematic of the air gap membrane distillation (AGMD) setup is shown in Fig. 1. AGMD has garnered considerable attention in recent years due to its high thermal efficiency and relatively low electrical energy consumption, positioning it as a promising solution for water desalination.

In this setup, the heated saline feed is delivered to the upper surface of a flat-sheet membrane

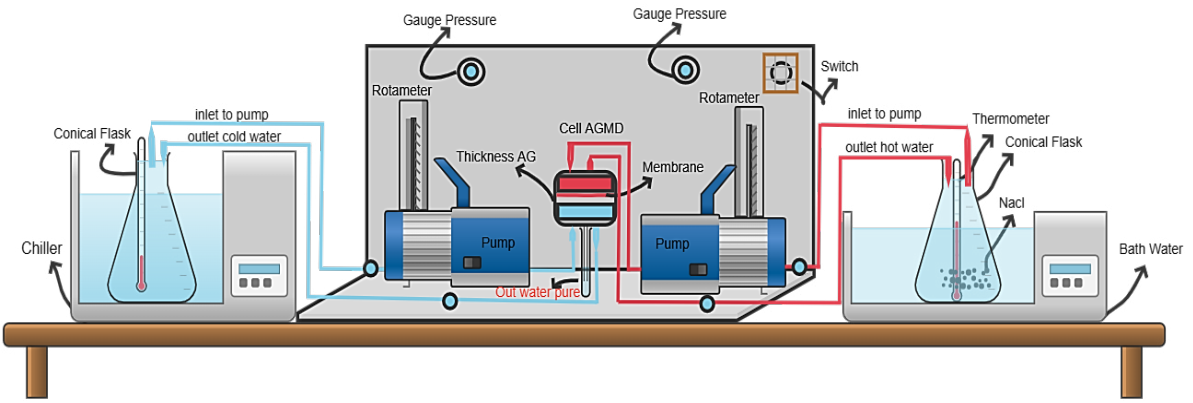

Fig. 1. The schematic of the evaluation of the membrane performance within the AGMD setup.

module via a peristaltic pump. The flow rate is controlled using a valve and monitored with a pressure gauge to ensure consistent operating conditions. As the feed water flows along the membrane surface, water vapor is generated and transported through the hydrophobic membrane pores, driven by the vapor pressure gradient across the membrane.

The vapor then passes through a quiescent layer of air between the membrane and a chilled condensing surface. When it gets to the cold, cold side, it condenses into liquid water. After reaching the cold side, the vapor condenses to a liquid, water. With its flow controlled and measured, the second peristaltic pump pumps cold water behind the condensation plate. The permeate (i.e., condensate) is collected at the outlet in a graduated measuring cylinder, and the temperature of the hot and cold inlets and outlets is continually recorded with digital sensors for accurate thermal control. The condensed water (permeate) is collected at the outlet with the graduated measuring cylinder, while temperatures at the hot and cold stream inlets and outlets are measured digitally by sensors to achieve accurate thermal control. The salinity concentration of the feed and permeate is monitored by a portable digital conductivity meter (TDS EC pH Temp Salinity Meter) (Kariman et al., 2025). The test is performed in steady-state and held for 3 h. The membrane module is made up of acrylic (Perspex) panels, selected for their chemical resistance, thermal stability, and ease of machining. Each of these internal chambers of the module is 7 cm x 7 cm with a depth of 1.5 cm. To evaluate the performance of the system, the following two parameters were determined: permeate flux (J) (kg/m².h) (Al-Harby et al., 2023) and salt rejection (R%) (Hardikar et al., 2023). They are calculated using the following equations:

$$J = \frac{V \times \rho}{A \times t} \qquad (1)$$

Where the permeate flux is represented in (kg/m².h), V is the freshwater volume (L), ρ is the water density (kg/L), t is the operational time (hour), and A is the area of the membrane.

$$R\% = \frac{C_1 - C_2}{C_1} \times 100 \qquad (2)$$

Where here, R is the salt retention, C1 is the feed concentration, and C2 is the concentration of the permeate.

The thickness of the air gab is effective in determining the performance of Air Gap Membrane Distillation (AGMD) systems. In terms of function, the air gap serves both as a barrier to mass transfer and as a thermal insulator between the membrane and the condensation

surface. This insulation helps minimize heat loss through conduction across the membrane (Shahu and Thombre, 2019). However, an increased air gap height offers more vapor diffusion resistance, and it will greatly decrease the permeate flux. Nevertheless, increasing the air gap thickness results in higher resistance to the vapor diffusion, which may reduce the permeate flux extensively (produces a negative correlation) (Matheswaran et al., 2007). It is important to carefully tune the thickness of the air gap because a smaller gap will decrease the diffusion resistance and improve mass transfer, and vice versa, to go beyond the right balance and get increased vapor flux simultaneously. An essential requirement for this is an accurate air gap thickness optimization. It is promoting the vapor transport effectively by keeping enough thermal insulation, necessary to achieve the best distillation performance corresponding to AGMD systems.

The feed temperature is generally acknowledged as the most critical parameter affecting the efficiency of membrane distillation (MD) units. This is mainly because the driving force for mass transfer in MD is the vapor pressure of the liquid, which increases steeply with temperature (according to Antoine's equation). And indeed, with an increasing feed temperature (if the temperature difference between the hot feed and the cold condensation surface remains constant), the vapor pressure at the hot side rises. These results in an enhanced vapor pressure drop across the membrane, which leads to the increase of vapor transport and eventually an increase of permeate flux (Nayeri and Mousavi, 2024). The performance of MD is extremely sensitive to thermal conditions, particularly the feed side; therefore, its temperature should be accurately controlled to keep it at the best condition.

The flow rates have a significant effect on the reaction. The feed flow rate in the membrane module serves for both heat and mass transfer. With the increase of flow rate, Reynolds number increases as well, and thinner convective heat and mass boundary layers are formed above the membrane surface. These thinner skins have lower transport process resistances and enhance the vapor pressure drop across the membrane. Thereby, a high feed flow rate, which is often associated with better mass transfer between vapor and permeate and improved permeate flux (Adewole et al., 2022). In this regard, the manipulation of the feed flow rate represents an efficient manner to enhance the overall productivity and performance of AGMD modules.

The salinity of the feed solution also has a beneficial effect on membrane distillation performance. As according to Raoult's Law, when the salt concentration increases, the vapor pressure of the solution decreases, thereby reducing the driving force for the mass transfer. In addition, accumulation of solute close to the membrane surface would lead to concentration polarization, defining a boundary layer at the top that hampers vapor transfer. This effect, along with the thermal boundary layer, increases the local viscosity and therefore leads to a higher barrier to mass transfer (Onsekizoglu, 2012). Although membrane distillation is more tolerant of high-salinity feeds than pressure-driven processes like reverse osmosis, the permeate flux generally declines as salt concentration increases.

RESULTS AND DISCUSSION

The results of membrane characterization showed that the surface morphology of the fabricated 15 wt.% recycled acrylic-based nanofibers membrane was investigated using scanning electron microscopy (SEM), as shown in Fig. 2. The SEM image reveals that the average fiber diameter was estimated to be 1.12 ± 0.28 μm, based on measurements of 100 individual fibers using ImageJ. The diameter distribution indicates consistent fiber formation ranging between 0.5 to 1.5 μm, which is a relatively broad distribution. Such fine fiber dimensions contribute to a high surface-area-to-volume ratio, which is beneficial for mass transfer in membrane distillation (MD) applications. The absence of beads and surface defects indicates a stable electrospinning process resulting in homogeneous fiber formation. The interconnected fibrous network is expected

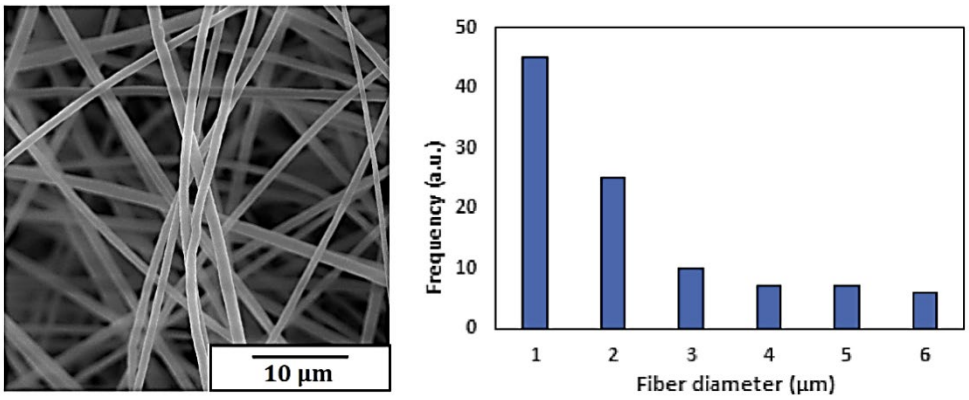

(a) (b)

Fig. 2. The surface morphology of the prepared recycled acrylic-based non-woven nanofibers membranes (A) the SEM image. (B) The histogram of the fiber diameter distribution.

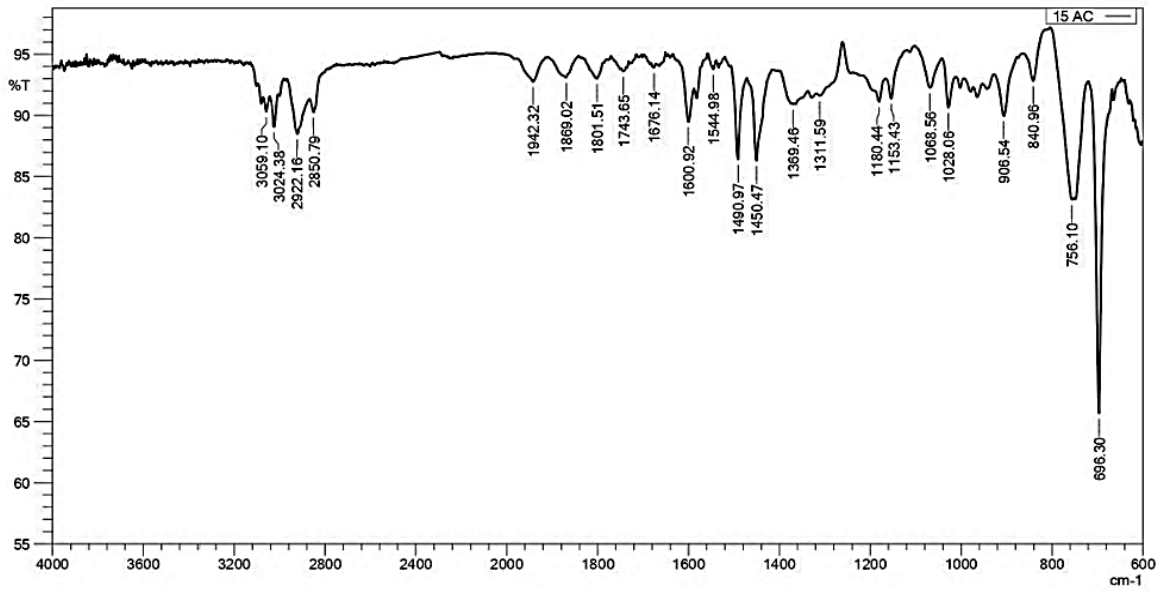

Fig. 3. The FTIR spectra of recycled acrylic-based nanofiber membranes.

to provide sufficient mechanical support while maintaining a high degree of hydrophobicity, critical for maintaining liquid-vapor separation. Moreover, the nanofibrous architecture allows for efficient vapor diffusion, potentially improving water flux while maintaining high salt rejection. The random orientation of fibers forms a highly porous structure, which is essential for promoting vapor transport while minimizing thermal conductivity and the risk of pore wetting. The FTIR spectrum (Fig. 3) displays characteristic absorption bands that confirm the chemical structure of PMMA. The peaks observed at 3024.38–3059.10 cm^{-1} are attributed to alkenic C–H stretching vibrations (Ren et al., 2021). While the strong absorptions in the 2995–2840 cm^{-1} range correspond to C–H stretching of $–CH_3$ and $–CH_2–$ groups, consistent with the aliphatic backbone of PMMA. A prominent peak at 1749.5 cm^{-1}, along with the broader range from 1676.14–1942.32 cm^{-1}, represents the C=O stretching vibration of ester groups, confirming the presence of acrylic components in the nanofiber membrane (Chakka et al., 2017). The bending vibrations of CH_2 and CH_3 groups are evident at 1460.9 and 1381.5 cm^{-1}, respectively. In the

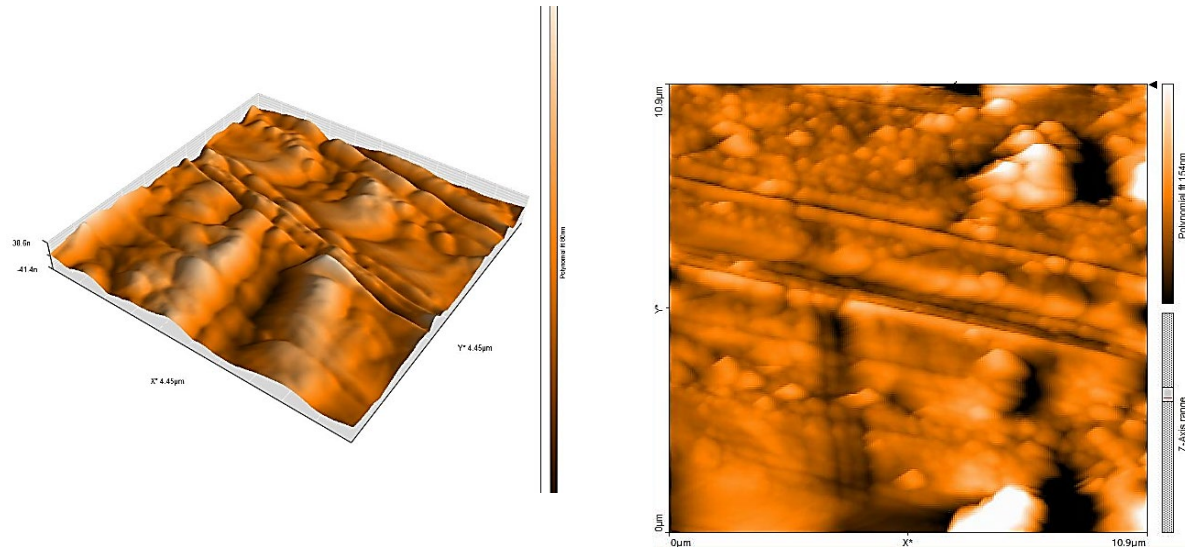

Fig. 4. Image of atomic force microscopy (AFM) of recycled acrylic-based nanofibers membrane.

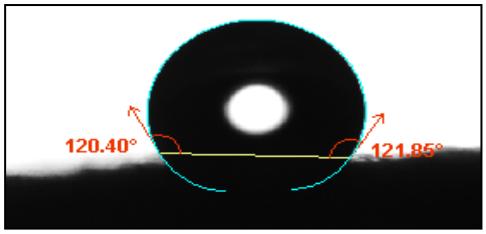

Fig. 5. The surface water contact angle of the fabricated recycled acrylic-based nanofibers membrane.

1260–1000 cm^{-1} region, multiple peaks correspond to C–O–C stretching vibrations of the ester moiety. Additionally, peaks in the 840–750 cm^{-1} region (including 756.1 and 698.3 cm^{-1}) are associated with out-of-plane bending of $–CH_2$ groups or side-chain vibrations. Collectively, these spectral features confirm the successful synthesis of PMMA nanofibers with intact ester functionalities and indicate the high chemical purity of the electrospun membrane, as no significant signals of degradation or contamination were detected.

Additionally, the AFM 2D and 3D images of the acrylic membrane, shown in Fig. 4, the surface roughness of the fabricated electrospun nanofiber membranes. The RA-based membrane was found to have an average surface roughness (Ra) of 132.9 nm and a mean diameter of 98.68 nm.

Therefore, the surface roughness of the electrospun membranes is related to the diameter of the nanofibers. It is noted that increasing roughness will make the hydrophobic membrane surface more hydrophobic.

Fig. 5 shows the image of contact angle measurement of a water droplet (WCA) on the membrane surface. The WCA was found to be 121.85°, indicating a highly hydrophobic surface. This value is considered suitable for membrane distillation (MD) applications. Hydrophobic surfaces exhibit strong water-repellent properties, making it difficult for water to wet the surface

To evaluate the potential of the fabricated membranes for brine water desalination, experiments were conducted using an Air Gap Membrane Distillation (AGMD) configuration. The study investigated the influence of key operational variables, including feed water temperature,

Table 1. Effect of air gap thickness on the permeation flux at 0.3L/min, 55 and 35 g/L NaCl.

Air Gap Thickness (mm)	Permeate Flux (kg/m²·h)	Salt Rejection (%)
6	5.8	99.998
9	3.2	99.999

feed flow rate, salt concentration, and air gap thickness, on permeate flux performance to identify optimal conditions for flux enhancement. The cold-side temperature and flow rate were maintained constant at 20 °C and 0.3 L/min, respectively. The hot-side inlet temperature was varied across three levels: 45 °C, 55 °C, and 65 °C. Additionally, hot-side flow rates were adjusted to 0.2, 0.3, and 0.4 L/min. The feed solutions used were NaCl brines at concentrations of 35, 70, and 140 g/L to simulate different levels of salinity. Throughout the experiments, the air gap thicknesses were varied to assess the impact on the desalination efficiency and permeate flux.

Air gap thickness plays a crucial role in determining the performance of AGMD systems. In this study, its effect was evaluated under constant conditions: a brine concentration of 35 g/L, coolant temperature of 15 °C, feed and coolant flow rates of 0.3 L/min, and a membrane thickness of 300 μm. The air gap thickness was varied from 9 mm to 6 mm using custom-designed acrylic panel inserts. As shown in Table 1, a reduction in air gap thickness led to a notable increase in permeate flux. This is primarily due to the decreased mass transfer resistance on the permeate side; thicker air gaps introduce greater resistance to vapor diffusion, thereby lowering flux. The selectivity of water vapor was found to be inversely proportional to air gap thickness, as a thinner gap enhanced both temperature and concentration gradients across the membrane (Matheswaran et al., 2007). Importantly, despite variations in air gap thickness, the membrane consistently exhibited excellent desalination performance, achieving salt rejection values ranging from 99.998% to 99.999%. Based on these findings, an air gap thickness of 6 mm was selected for the remainder of the experiments in this study.

The influence of feed temperature on permeate flux was examined under controlled conditions, with a brine concentration of 35 g/L, a coolant temperature of 15 °C, a coolant flow rate of 0.3 L/min, a feed flow rate of 0.3 L/min, a membrane thickness of 300 μm, and an air gap thickness of 6 mm. The feed temperature was in the range of 45 to 65°C, with all other parameters kept the same. As shown in Fig. 6, with all other parameters unchanged, as the feed temperature increased, an increase in flux of the distillate was observed. This was due to a significant increase in the saturated vapor pressure of water, and an improvement of the driving force for water-vapor transport through the membrane. This relationship is quantified by the Antoine equation, which characterizes how vapor pressure increases with liquid temperature, determining the mass transfer in MD operations (Safi et al., 2020). Even though high feed temperature proved to increase permeate flux, some attention should be given, on one hand, to the increased energy consumption in warming up feed solution and, on the other, to the deleterious effect of high temperature on membranes' lifetime. Higher feed temperatures enhance the vapor pressure difference across the membrane and consequently enhance the driving force of mass transfer in the membrane distillation (MD) process. This thermal gain requires more energy supply, especially at relatively high temperatures above 60 °C, with an increasing massive heating load occurring (Al-Sairfi et al., 2023). Maximum flux was achieved at 65 °C, and this temperature can be considered as the optimum operation in the present study, taking also into account its potential use in desalination plants. At a temperature of 65°C, it offered an effective compromise between performance and energy efficiency, delivering high water recovery, thus maintaining a relatively reasonable thermal energy requirement, thus supporting its suitability for efficient brine treatment using the AGMD technology.

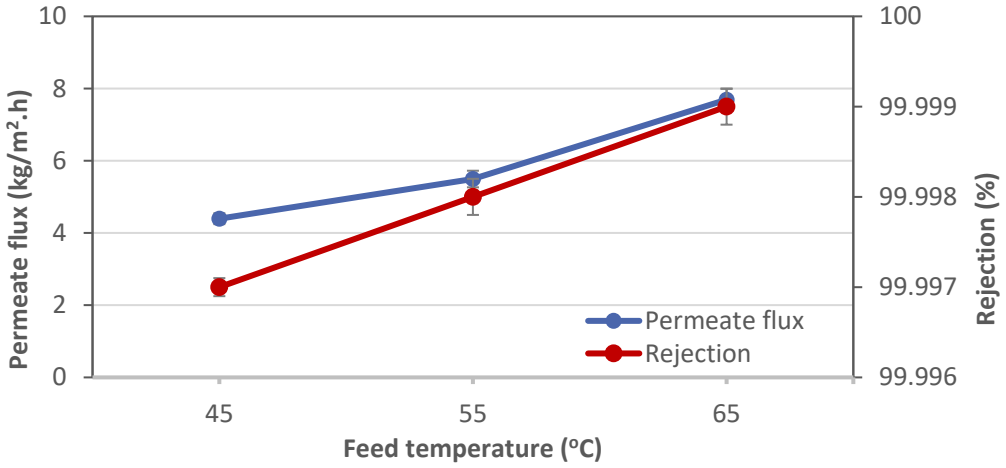

Fig. 6. The influence of feed temperature on the permeate flux of RA-based membrane using the AGMD configuration at 0.3 L/min, 6 mm and 35 g/L NaCl.

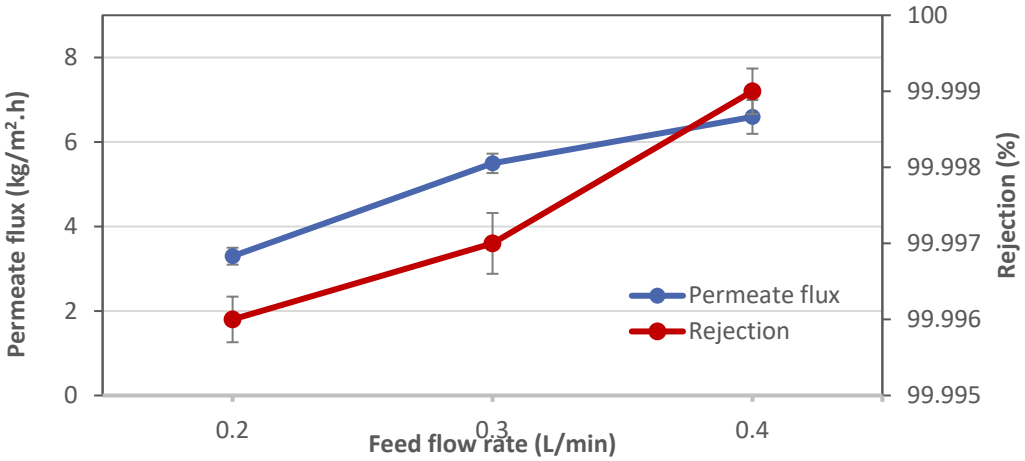

Fig. 7. The influence of feed flow rate on the permeate flux of RA-based membrane at 55°C, 6 mm and 35 g/L NaCl solution using the AGMD configuration.

The feed flow rate is a critical operating variable that significantly influences the performance of membrane distillation (MD) systems. To estimate its impact on the AGMD setup, experiments were conducted under the previously described conditions. As shown in Fig. 7, increasing the feed flow rate from 0.2 to 0.4 L/min resulted in a nearly linear increase in distillate flux. These improvements can be attributed to increased turbulence within the flow channel, which promotes better mixing and mass transfer across the 15 wt.% acrylic nanofiber membrane. The rise in Reynolds number associated with higher flow rates leads to a reduction in the thickness of the hydrodynamic boundary layer, improving the heat transfer coefficient and thereby minimizing the temperature polarization effect on the feed side.

This finally results in a more effective driving force for vapor transport. Particularly, because of increased feed flow rates, the fabricated membranes maintained excellent separation performance, with salt rejection values ranging from 99.996% to 99.999% across the tested flow rates (Said et al., 2020).

The salt concentration in the feed solution is a vital component influencing the performance of AGMD systems. In this study result, the impact of feed salinity was evaluated by different the salt concentration from 35 to 140 g/L while keeping all other operating parameters

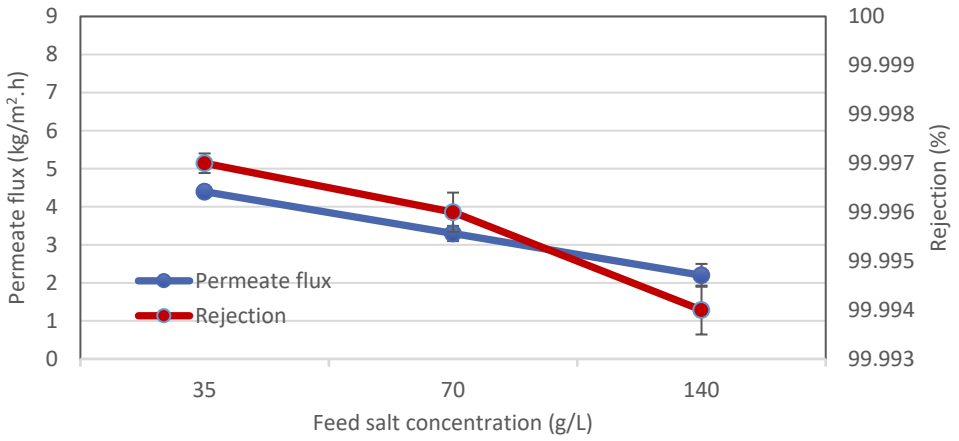

Fig. 8. The effect of NaCl concentration on the permeate flux of recycled RA-based membrane on the surface at 55℃, 6 mm and 0.3 L/min.

Table 2. Comparison with other studies of membrane researchers' operating conditions and permeate flux in AGMD

Membrane name	Temp. of feed (℃)	Flow rate of feed (L/min)	Conc. of feed (g/L)	Air gap thickness (mm)	Time of exp. (h)	Permeate flux (kg/m²·h)	Salt Rejection (%)	Ref.
PVDF-co-HEP+graphene	40	0.2	35	3	60	22.9	~100	(Woo et al., 2016)
PVDF/GO-APTS	40	0.5	3.5	2	15	10.7	~100	(Kebria et al., 2020)
PVDF	40	0.35	60	2	600	4.2	99.9	(Feng et al., 2008)
FGO-4/PVDF	40-60	0.16	35	4	8	5.33-21.43	99.9	(Xie et al., 2024)
Waste acrylic material (PMMA)	45-65	0.3	35	6	24	4.5-7.65	99.999	Present work

constant. As shown in Fig. 8, the distillate flux was highest at the lowest salt concentration and decreased significantly as the salt concentration increased. This decline in performance can be attributed to several factors. First, as salt concentration rises, the vapor pressure of the feed solution decreases, thereby reducing the driving force for mass transfer. Second, concentration polarization near the membrane surface may increase, further hindering vapor transport. Additionally, high salinity levels may promote surface fouling, which can reduce membrane efficiency over time. Despite the reduction in flux, approximately 60 % as the salt concentration increased from 35 to 140 g/L, the fabricated hydrophobic membranes maintained excellent salt rejection capabilities, with values ranging from 99.998% to 99.994%, indicating their strong potential for high-salinity desalination applications (Alftessi et al., 2022).

The RA-based membrane demonstrates competitive AGMD performance in an air gap thickness of 6 mm compared to other previously reported membranes (shown in Table 2), owing to its highly porous nanofibrous structure with interconnected pores that facilitate vapour transport.

Additionally, water contact angle measurements exceeding 121° indicate excellent hydrophobicity, which is essential for effective liquid–vapor separation and confirms the important rule that recycled acrylic-based nanofiber membranes are environmentally sustainable and also highly effective for cost-effective (economical), high-salinity brine desalination in AGMD. The high-water flux of 22.9 Kg/m².h and nearly 100% salt removal were achieved by the PVDF-HFP/graphene nanofibrous membrane in a 3 mm air gap, further demonstrating the potential in MD-based desalination and water treatment may be attributed to the excellent inherent hydrophobicity of the PVDF-HFP polymer (WCA value of 142.3° for the pristine

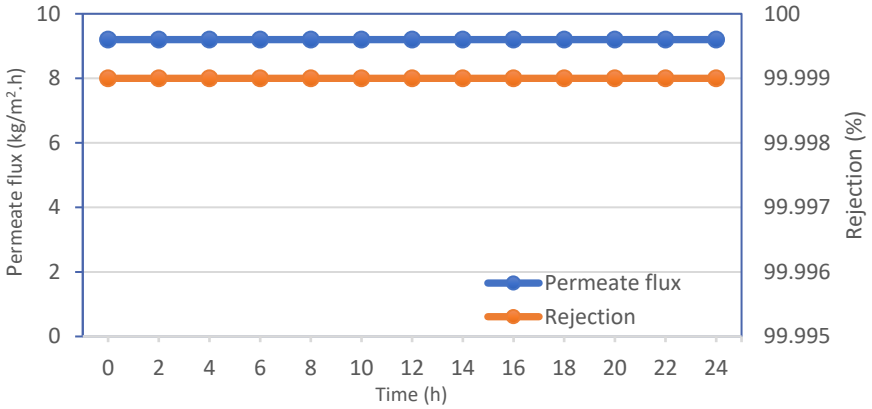

Fig. 9. The RA-base nanofibers membrane performance (permeate flux and salt rejection) over 24 hours under the best operating conditions of 65°C, 6 mm, 35 (g/L), and 0.4 (L/min).

PVDF-HFP membrane) as well as the high porosity of 88.7% (Woo et al., 2016). Compared to another membrane, the RA material is more inexpensive and practical for further modification or grafting because of the available surface functional groups.

Membrane performance (at best operating parameters), including operational stability over 24 hours, is a crucial factor in assessing the suitability of a new membrane for MD applications. Generally, it can be identified that membrane wettability and permeate flux are considered the main goals for improving the membrane fabrication technique. We conducted the operation using the best operating conditions obtained with a feed temperature of 65°C, a feed rate of 0.4 L/min, a coolant temperature of 15°C for the AGMD (thickness of 6 mm), and the feed solution prepared by dissolving 35 g/L of NaCl in distilled water. The MD test was carried out for 24 hours, and the membrane performance was compared depending on the permeate flux and salt rejection. The RA-based fabricated electrospun membrane with high performance was selected and explained before due to its high hydrophobicity, so no significant changes in the permeate flux were observed during the period of 24 hr., maintaining a flux of 9.2 kg/m²·h and high salt rejection rates of 99.999%, as shown in Fig.9. The nanofiber membrane showed no observable signs of wetting, fouling, or structural degradation and maintained its hydrophobicity and mechanical integrity under operational conditions, sustaining the vapor pressure difference across the membrane, making it a good candidate for AGMD applications, with an uncomplicated fabrication technique used via electrospinning. Despite efforts to develop highly non-wetting membranes with superhydrophobic surfaces, minimal performance stability is still a real challenge for MD.

CONCLUSIONS

This study demonstrated the successful fabrication of electrospun nanofiber membranes using recycled acrylic as a sustainable polymer source for Air Gap Membrane Distillation (AGMD) applications. The membranes exhibited favorable morphological and physicochemical characteristics, including a uniform and highly porous fiber network, notable surface roughness, and strong hydrophobicity, with water contact angles exceeding 121°. FTIR analysis confirmed the preservation of functional groups, indicating good chemical integrity and thermal stability. The membranes were evaluated in a custom-designed AGMD system under a range of operating conditions, including feed temperatures between 45 and 65 °C, flow rates of 0.2 to 0.4 L/min, salt concentrations from 35 to 140 g/L, and air gap thicknesses of 6 to 9 mm. The highest permeate

flux (9.2 kg/m²·h) was recorded at 65 °C and 0.4 L/min and was maintained steadily over a 24-hour period. Performance analysis revealed that increases in feed temperature and flow rate enhanced flux, primarily by increasing vapor pressure and mitigating temperature polarization. In contrast, larger air gap thicknesses and higher salt concentrations contributed to lower flux due to elevated mass transfer resistance and concentration polarization effects. Nonetheless, the membranes consistently delivered high salt rejection rates, ranging from 99.994% to 99.999%, underscoring their reliability and selectivity even under challenging conditions. Overall, the findings highlight the potential of recycled acrylic-based nanofiber membranes as an effective and environmentally responsible option for desalinating high-salinity brines using AGMD. This work supports the broader goal of developing sustainable, cost-effective membrane materials for future water treatment technologies.

GRANT SUPPORT DETAILS

The present research did not receive any financial support.

CONFLICT OF INTEREST

The authors declare that there is no conflict of interest regarding the publication of this manuscript. In addition, the ethical issues, including plagiarism, informed consent, misconduct, data fabrication and/ or falsification, double publication and/or submission, and redundancy, have been completely observed by the authors.

LIFE SCIENCE REPORTING

No life science threat was practiced in this research.

REFERENCES

Alftessi, S. A., Othman, M. H. D., Adam, M. R. B., Farag, T. M., Tai, Z. S., Raji, Y. O., & Bakar, S. A. (2022). Hydrophobic silica sand ceramic hollow fiber membrane for desalination via direct contact membrane distillation. Alexandria Engineering Journal, 61(12), 9609-9621.https://doi.org/10.1016/j.aej.2022.03.044

Abdulhussain, R., Adebisi, A., Conway, B.R., & Asare-Addo, K., (2023). Electrospun nanofibers: Exploring process parameters, polymer selection, and recent applications in pharmaceuticals and drug delivery. J. Drug Deliv Sci Technol., 90. https://doi.org/10.1016/j.jddst.2023.105156

Abid, M. Bin, Wahab, R.A., Salam, M.A., Gzara, L., & Moujdin, I.A. (2023). Desalination technologies, membrane distillation, and electrospinning, an overview. Heliyon, 9 (2). https://doi.org/10.1016/j.heliyon.2023.e12810

Adewole, J. K., Al Maawali, H. M., Jafary, T., Firouzi, A., & Oladipo, H. (2022). A review of seawater desalination with membrane distillation: material development and energy requirements. Water Supply, *22*(12), 8500-8526. https://doi.org/10.2166/ws.2022.337

Albiladi, A., Gzara, L., Organji, H., Alkayal, N.S., & Figoli, A. (2023). Electrospun Poly (Vinylidene Fluoride-Co-Hexafluoropropylene) Nanofiber Membranes for Brine Treatment via Membrane Distillation. Polymers (Basel)., 15. https://doi.org/10.3390/polym15122706

Al-Harby, N.F., El Batouti, M., Elewa, M.M. (2023). A Comparative Analysis of Pervaporation and Membrane Distillation Techniques for Desalination Utilising the Sweeping Air Methodology with Novel and Economical Pervaporation Membranes. Polymers (Basel)., 15. https://doi.org/10.3390/polym15214237

Ali, U., Karim, K. J. B. A., & Buang, N. A. (2015). A review of the properties and applications of poly (methyl methacrylate)(PMMA). Polymer Reviews., 55(4), 678-705. https://doi.org/10.1080/15583724.2015.1031377

Alkarbouly, S.M., & Waisi, B.I. (2022). Fabrication of Electrospun Nanofibers Membrane for Emulsified Oil Removal from Oily Wastewater. Baghdad Science Journal., 19, 1238–1248. https://doi.org/10.21123/bsj.2022.6421

Al-Sairfi, H., Koshuriyan, M.Z.A., Ahmed, M. (2023). Performance feasibility study of direct contact membrane distillation systems in the treatment of seawater and oilfield-produced brine: the effect of hot- and cold-channel depth. Desalination Water Treat., 313, 26–36. https://doi.org/10.5004/dwt.2023.29942

Chakka, A.K., Muhammed, A., Sakhare, P.Z., & Bhaskar, N. (2017). Poultry Processing Waste as an Alternative Source for Mammalian Gelatin: Extraction and Characterization of Gelatin from Chicken Feet Using Food Grade Acids. Waste Biomass Valorization., 8, 2583–2593. https://doi.org/10.1007/s12649-016-9756-1

Chigome, S., Darko, G., & Torto, N. (2011). Electrospun nanofibers as sorbent material for solid phase extraction. Analyst., 136(14), 2879-2889. https://doi.org/10.1039/c1an15228a

Coates, J. (2000). Interpretation of Infrared Spectra, A Practical Approach, in: Encyclopedia of Analytical Chemistry. Wiley. https://doi.org/10.1002/9780470027318.a5606

Criscuoli, A. (2021). Membrane distillation process. Membranes (Basel)., 11(2), 144. https://doi.org/10.3390/membranes11020144

Defor, C., Chou, & S.F. (2024). Electrospun polytetrafluoroethylene (PTFE) fibers in membrane distillation applications. AIMS Mater Sci., 11, 1179–1198. https://doi.org/10.3934/MATERSCI.2024058

Fang, J., Zhang, L., Sutton, D., Wang, X., & Lin, T. (2012). Needleless melt-electrospinning of polypropylene nanofibres. Journal of nanomaterials, 2012(1), 382639. https://doi.org/10.1155/2012/382639

Feng, C., Khulbe, K.C., Matsuura, T., Gopal, R., Kaur, S., Ramakrishna, S., & Khayet, M. (2008). Production of drinking water from saline water by air-gap membrane distillation using polyvinylidene fluoride nanofiber membrane. J. Memb Sci., 311, 1–6. https://doi.org/10.1016/j.memsci.2007.12.026

Fernandes, I.S., Domingos, M.G., Costa, M.F., Santos, R.J., & Lopes, J.C.B. (2025). Hydrate-based desalination process using CO_2 as hydrate forming agent–Modelling and techno-economic analysis. Desalination., 599. https://doi.org/10.1016/j.desal.2024.118426

Hardikar, M., Felix, V., Presson, L.K., Rabe, A.B., Ikner, L.A., &Achilli, A. (2023). Pore Flow and Solute Rejection in Pilot-Scale Air-Gap Membrane Distillation. J. Memb Sci., 676, 121544. https://doi.org/10.1016/j.memsci.2023.121544

Huang, Z.M., Zhang, Y.Z., Kotaki, M., Ramakrishna, S. (2003). A review on polymer nanofibers by electrospinning and their applications in nanocomposites. Compos. Sci Technol., 63, 2223–2253. https://doi.org/10.1016/S0266-3538(03)00178-7

Islam, M. S., Ang, B. C., Andriyana, A., & Afifi, A. M. (2019). A review on fabrication of nanofibers via electrospinning and their applications. SN Applied Sciences, 1(10), 1248. https://doi.org/10.1007/s42452-019-1288-4

Kariman, H., Mohammed, H. A., Zargar, M., & Khiadani, M. (2025). Performance comparison of flat sheet and hollow fibre air gap membrane distillation: A mathematical and simulation modelling approach. Journal of Membrane Science, 721, 123836. https://doi.org/10.1016/j.memsci.2025.123836

Kebria, M. R. S., Rahimpour, A., Salestan, S. K., Seyedpour, S. F., Jafari, A., Banisheykholeslami, F., & Kiadeh, N. T. H. (2020). Hyper-branched dendritic structure modified PVDF electrospun membranes for air gap membrane distillation. Desalination, 479, 114307. https://doi.org/10.1016/j.desal.2019.114307

Liao, S. W., Lin, C. I., & Wang, L. H. (2011). Kinetic study on lead (II) ion removal by adsorption onto peanut hull ash. Journal of the Taiwan Institute of Chemical Engineers, 42(1), 166-172. https://doi.org/10.1016/j.jtice.2010.04.009

Liu, S., Jun, S. C., Zhang, S., Wang, F., Yu, J., & Ding, B. (2024). Advancements in electrospun nanofibrous membranes for improved waterproofing and breathability. Macromolecular Materials and Engineering, 309(9), 2300312. https://doi.org/10.1002/mame.202300312

Matheswaran, M., Kwon, T. O., Kim, J. W., & Moon, I. S. (2007). Factors affecting flux and water separation performance in air gap membrane distillation. Journal of Industrial and Engineering Chemistry-Seoul-, 13(6), 965.

Navarro-Tovar, R., Qiu, B., Martin, P., Gorgojo, P., & Perez-Page, M. (2025). Advanced desalination performance using PVDF electrospun nanofiber membranes across multiple membrane distillation configuration. Desalination, 598, 118425. https://doi.org/10.1016/j.desal.2024.118425

Nayeri, D., & Mousavi, S. A. (2024). A critical review on the effect of silanization on the ceramic

membrane distillation (CMD): performance, operational factors, and characterization. Applied Water Science, 14(6), 114. https://doi.org/10.1007/s13201-024-02178-3

Onsekizoglu, P. (2012). Membrane Distillation: Principle, Advances, Limitations and Future Prospects in Food Industry, (p. 282). IntechOpen.

Ren, J., Wang, X., Zhao, L., Li, M., & Yang, W. (2021). Effective removal of dyes from aqueous solutions by a gelatin hydrogel. Journal of Polymers and the Environment, 29(11), 3497-3508. https://doi.org/10.1007/s10924-021-02136-z

Safi, N.N., Ibrahim, S.S., Zouli, N., Majdi, H.S., Alsalhy, Q.F., Drioli, E., Figoli, A. (2020). A systematic framework for optimizing a sweeping gas membrane distillation (SGMD). Membranes (Basel), 10, 1–18. https://doi.org/10.3390/membranes10100254

Safi, N.N., & Waisi, B.I. (2023). Preparation of electrospun double-layer PVDF:PMMA membrane non-woven nanofibers for desalination by membrane distillation process. Desalination Water Treatment, 314, 49–58. https://doi.org/10.5004/dwt.2023.30063

Shahu, V. T., & Thombre, S. B. (2019). Air gap membrane distillation: A review. Journal of Renewable and Sustainable Energy, 11(4). https://doi.org/10.1063/1.5063766

Shahzad, M.W., Burhan, M., Ybyraiymkul, D., & Ng, K.C. (2019). Desalination processes' efficiency and future roadmap. Entropy, 21. https://doi.org/10.3390/e21010084

Soumbati, Y., Bouatou, I., Abushaban, A., Belmabkhout, Y., & Necibi, M. C. (2025). Review of membrane distillation for desalination applications: Advanced modeling, specific energy consumption, and water production cost. Journal of Water Process Engineering, 71, 107296. https://doi.org/10.1016/j.jwpe.2025.107296

Subbiah, T., Bhat, G. S., Tock, R. W., Parameswaran, S., & Ramkumar, S. S. (2005). Electrospinning of nanofibers. Journal of Applied Polymer Science, 96(2), 557-569. https://doi.org/10.1002/app.21481

Woo, Y. C., Tijing, L. D., Shim, W. G., Choi, J. S., Kim, S. H., He, T., Drioli, E., & Shon, H. K. (2016). Water desalination using graphene-enhanced electrospun nanofiber membrane via air gap membrane distillation. Journal of Membrane Science, 520, 99-110. https://doi.org/10.1016/j.memsci.2016.07.049

Xie, Y., Yu, L., & Yu, Y. (2024). Improved desalination performance of fluorinated graphene oxide blended PVDF electrospun nanofiber membrane for air gap membrane distillation. Desalination Water Treatment, 317. https://doi.org/10.1016/j.dwt.2024.100184

Zhang, M., Ahmed, A., & Xu, L. (2023). Electrospun nanofibers for functional food packaging application. Materials, 16(17), 5937. https://doi.org/10.3390/ma16175937

Zhang, Z., Wu, X., Kou, Z., Song, N., Nie, G., Wang, C., Verpoort, F. & Mu, S. (2022). Rational design of electrospun nanofiber-typed electrocatalysts for water splitting: A review. Chemical Engineering Journal, 428, 131133. https://doi.org/10.1016/j.cej.2021.131133

Zhang, Z., Wu, X., Kou, Z., Song, N., & Nie, G. (2022) Rational design of electrospun nanofiber-typed electrocatalysts for water splitting: A review. Chemical Engineering Journal, 428, p.131133.